

Varying Eu²⁺ magnetic order by chemical pressure in EuFe₂(As_{1-x}P_x)₂

S. Zapf, D. Wu, L. Bogani, H. S. Jeevan, Philipp Gegenwart, M.
Dressel

Angaben zur Veröffentlichung / Publication details:

Zapf, S., D. Wu, L. Bogani, H. S. Jeevan, Philipp Gegenwart, and M. Dressel. 2011.
"Varying Eu²⁺ magnetic order by chemical pressure in EuFe₂(As_{1-x}P_x)₂."
Physical Review B 84 (14): 140503(R).
<https://doi.org/10.1103/physrevb.84.140503>.



Varying Eu^{2+} magnetic order by chemical pressure in $\text{EuFe}_2(\text{As}_{1-x}\text{P}_x)_2$

S. Zapf,¹ D. Wu,¹ L. Bogani,¹ H. S. Jeevan,² P. Gegenwart,² and M. Dressel¹

¹*Physikalisches Institut, Universität Stuttgart, Pfaffenwaldring 57, D-70550 Stuttgart, Germany*

²*Physikalisches Institut, Universität Göttingen, Friedrich-Hund-Platz 1, D-37077 Göttingen, Germany*

(Received 11 March 2011; revised manuscript received 26 July 2011; published 13 October 2011)

Based on low-field magnetization measurements on a series of single crystals, we present a scheme of the Eu^{2+} spin alignment in $\text{EuFe}_2(\text{As}_{1-x}\text{P}_x)_2$. We explain observations of the Eu^{2+} ordering previously reported, reconciling different existing phase diagrams. The magnetic moments of the Eu^{2+} ions are slightly canted, yielding a ferromagnetic contribution along the c direction that becomes stronger with pressure, until superconductivity sets in. The spin-density wave as well as the superconducting phase coexist with an antiferromagnetic interlayer coupling of the canted spins. Reducing the interlayer distance finally leads to a ferromagnetic Eu^{2+} interlayer coupling and to the suppression of superconductivity.

DOI: [10.1103/PhysRevB.84.140503](https://doi.org/10.1103/PhysRevB.84.140503)

PACS number(s): 74.70.Xa, 74.62.Fj, 74.25.Ha, 75.30.Gw

I. INTRODUCTION

With the discovery of superconductivity in iron pnictides, a new approach was taken toward understanding the mechanism of high-temperature superconductivity. Magnetism seems to be the crucial factor determining the physical properties, as superconductivity emerges with the suppression of the spin-density-wave (SDW) ordering in the FeAs layers.¹ The ternary 122 compounds quickly advanced as the model systems due to the availability of good single crystals. EuFe_2As_2 is an outstanding member of the 122 series with a maximum critical temperature $T_c = 32$ K in $\text{Eu}_{0.5}\text{K}_{0.5}\text{Fe}_2\text{As}_2$,² because in addition to the antiferromagnetic (AFM) order of the itinerant electrons at $T_{\text{SDW}} = 189$ K, magnetic order of the localized Eu^{2+} ions is observed at low temperatures.³ Eu^{2+} possesses a large magnetic moment and exhibits a so-called “A-type” AFM ordering below $T_N = 19$ K, meaning that the Eu^{2+} moments align ferromagnetically along the a axis and antiferromagnetically along the c axis.^{4–7} The interplay of the second magnetic ordering with the SDW draws increasing attention.^{8,9}

Charge-carrier doping,^{2,10,11} isovalent P substitution on the As site,^{12,13} and physical pressure^{14–16} change the Eu^{2+} ordering as well as electronic properties of the system, eventually leading to superconductivity. One interesting signature of these superconductors is a resistivity reentrance below T_c in the range of the Eu^{2+} ordering temperature, observed for example in $\text{Eu}(\text{Fe}_{0.89}\text{Co}_{0.11})_2\text{As}_2$,¹¹ $\text{EuFe}_2(\text{As}_{0.7}\text{P}_{0.3})_2$,¹² and EuFe_2As_2 under pressure.^{14–16} Thus the Eu^{2+} ordering has noticeable impact on superconductivity in the FeAs layers, revealing an extraordinary possibility to study the interplay between magnetism and superconductivity.¹⁷

It is therefore quite surprising that, at present, no clear picture exists how the Eu^{2+} ordering changes with doping or pressure. Furthermore, it is still under debate which kind of Eu^{2+} magnetic order coexists with superconductivity.^{8,13} In the following, we concentrate on $\text{EuFe}_2(\text{As}_{1-x}\text{P}_x)_2$ and discuss the influence of chemical pressure on the alignment of the Eu^{2+} magnetic moments. We conclude that the Eu^{2+} spins are canted along the c axis, causing an appreciable ferromagnetic (FM) contribution that increases with the suppression of the SDW. In addition to this canting, the interlayer coupling changes from AFM to FM, when superconductivity is suppressed. Our

scheme explains the apparent discrepancies in phase diagrams of Eu^{2+} magnetic ordering.^{8,13}

II. EXPERIMENTAL RESULTS

The $\text{EuFe}_2(\text{As}_{1-x}\text{P}_x)_2$ single crystals used in this study were synthesized and characterized as previously described.¹³ Optical investigations on crystals with $x = 0$ and 0.18 have been already reported.^{18,19} Here we describe the magnetic behavior of $x = 0, 0.055, 0.12,$ and 0.35 single crystals, measured with a Quantum Design MPMS-XL superconducting quantum interference device. We provide a characterization as a function of temperature (T) and magnetic field (H) for the main crystallographic directions. EuFe_2As_2 has orthorhombic symmetry with a and b axis virtually identical.²⁰ Even though twinning did not allow us a characterization in the ab plane, neutron and x-ray scattering data indicate that the Eu^{2+} moments align along the a direction.^{4–7}

Figure 1 shows the temperature-dependent magnetization for $x = 0.12$ and $H = 20$ Oe, measured parallel and perpendicular to the ab plane, as well as for $x = 0, 0.055,$ and 0.35 and $H \parallel c$. While at elevated temperatures ($T > T_{\text{SDW}}$ for $x = 0, 0.055,$ and 0.12) the paramagnetic regime can be, similar to the parent compound, described by the Curie-Weiss law,¹⁸ the magnetization behavior at low temperatures differs significantly. For $x = 0, 0.055,$ and 0.12, a cusp at $T_N = 19, 18,$ and 16 K, respectively, evidences AFM order of the Eu^{2+} spins. Nevertheless, for $x = 0.12$, we find at low temperatures a distinct difference between the field-cooled (FC) and zero-field-cooled (ZFC) curves (especially for $H \parallel c$) that becomes more pronounced as P substitution increases.¹³ For $x = 0.35$, FM order develops below $T_m = 21$ K for both field directions (see also Fig. 3). (Resistivity measurements do not show superconductivity for this sample.)

Furthermore, we measured the field dependence of the magnetization for $H \parallel ab$ and $H \parallel c$. The complete magnetization versus field curve has already been discussed^{3,8} and here we concentrate on low fields. Figure 2 displays the results obtained for $\text{EuFe}_2(\text{As}_{0.88}\text{P}_{0.12})_2$ at low temperatures. We observe a clear hysteresis for $H \parallel c$. (For $H \parallel ab$, only a much smaller hysteresis is observed, which is likely caused by our limited precision in crystal alignment.) To follow the opening of the

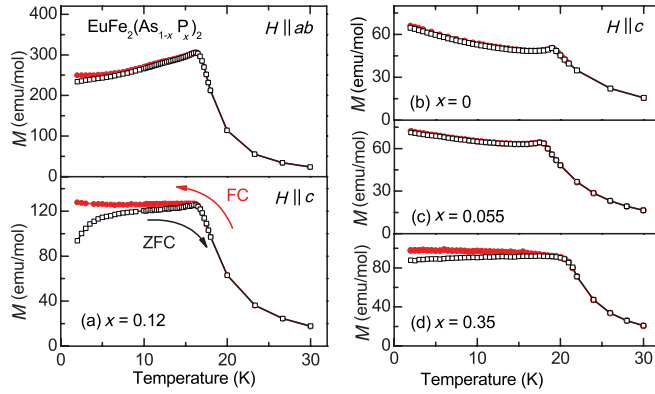


FIG. 1. (Color online) $\text{EuFe}_2(\text{As}_{1-x}\text{P}_x)_2$: ZFC (black open squares) and FC (solid red circles) magnetization curves measured in $H = 20$ Oe and (a) for $x = 0.12$ parallel (upper panel) and perpendicular (lower panel) to the ab plane, for (b) $x = 0$, (c) $x = 0.055$, and (d) $x = 0.35$ in $H \parallel c$.

hysteresis, we plot in Fig. 2(b) the difference ΔM_c between the magnetization curves acquired by sweeping the field down and up (i.e., the hysteresis height) for $H \parallel c$. ΔM_c decreases on raising the temperature, until the hysteresis vanishes at $T_N = 16$ K and it is instructive to compare this trend with the difference between the ZFC and FC curves at the same field. The two trends coincide, demonstrating the development of magnetic ordering.

Figure 3 displays the isothermal magnetization at 2 K and ΔM for the compositions $x = 0, 0.055$, and 0.35 . We are not able to resolve a hysteresis for $x = 0$, while for $x = 0.055$ the hysteresis height gives a very small, but positive signal for $H \parallel c$. For $x = 0.35$, one observes a distinct hysteresis opening for $H \parallel ab$, as well as a small opening for $H \parallel c$. The different temperature dependence of ΔM_{ab} and ΔM_c indicates two unequal FM mechanisms for the two crystal directions.

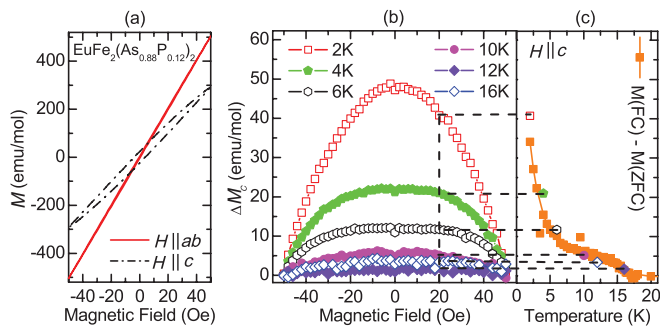


FIG. 2. (Color online) $\text{EuFe}_2(\text{As}_{0.88}\text{P}_{0.12})_2$: (a) Isothermal magnetization versus external magnetic field applied parallel (red solid line) and perpendicular (black dashed line) to the ab plane at $T = 2$ K. A clear hysteresis can be observed for $H \parallel c$ (but can also be identified for $H \parallel ab$). (b) Height of the hysteresis, measured with $H \parallel c$ for different fields and temperatures. (c) Temperature dependence of the difference between the ZFC and FC curves shown in Fig. 1(a) (lower panel). This difference can be compared to the hysteresis height at $H = 20$ Oe shown in (b). The broken lines are a guide to the eye to stress the correlation between the two trends.

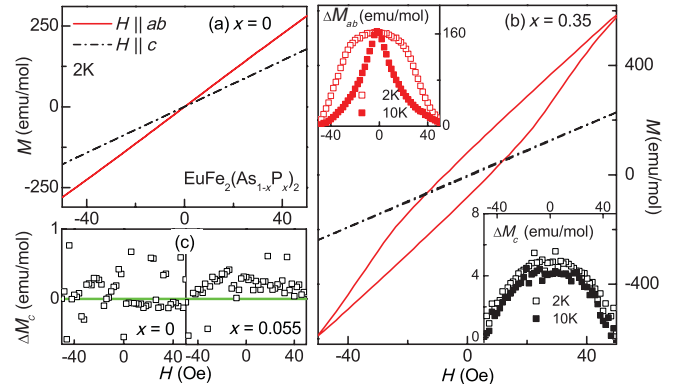


FIG. 3. (Color online) $\text{EuFe}_2(\text{As}_{1-x}\text{P}_x)_2$: Isothermal magnetization versus external magnetic field applied parallel (red solid lines) and perpendicular (black dashed lines) to the ab plane at $T = 2$ K for (a) $x = 0$ and (b) $x = 0.35$; (c) corresponding hysteresis height ΔM_c for $x = 0$ and $x = 0.055$ in $H \parallel c$. (a) While no hysteresis can be observed for $x = 0$, (b) in the case of $x = 0.055$, ΔM_c gives a very small signal above zero, indicated by the green line. For $x = 0.35$, one observes a distinct hysteresis for $H \parallel ab$ as well as a small hysteresis for $H \parallel c$ with a different temperature behavior. The insets in (b) show the hysteresis heights ΔM_{ab} and ΔM_c .

III. DISCUSSION

Combining our present and previous¹³ magnetization measurements with Ref. 8, we conclude that the Eu^{2+} magnetic moments change their alignment under pressure as displayed in Fig. 4. At low P concentration, the spins orient along the a direction, but basically reverse the direction in adjacent ab planes.⁴⁻⁷ More precisely, one observes canted AFM causing a small FM component of the moments in c direction that is usually neglected in discussions. Mössbauer studies reveal a steep increase of this canting angle with increasing P substitution until the Eu spins are aligned almost perpendicular to the ab plane when superconductivity sets in.⁸ We show that this canting leads in magnetic susceptibility measurements to a FM signal along the c axis, i.e., a hysteretic behavior, as it is shown for our $x = 0.12$ single crystal. The fact that in the parent compound the hysteresis cannot be resolved is consistent with an extremely small spin canting, which becomes slowly more pronounced ($x = 0.055$). For $x = 0.35$, one observes canting along c as well as FM interlayer coupling.

The hysteresis loops observed in our single crystal measurements for $H \parallel c$ constitute the key to reconcile the various phase diagrams of Eu 122 pnictides proposed in literature.^{8,13} Since contributions from the c direction are unavoidable in polycrystalline samples, a hysteresis is always seen as soon as the canting of the spins is sufficiently pronounced. In the following, we compare the phase diagram of our previous work (based on single crystal measurements)¹³ with that of Nowik *et al.* (based on polycrystalline samples).⁸ We observe AFM Eu^{2+} order in the superconducting phase, whereas the latter group claims the coexistence of FM and superconductivity. The statements do not contradict each other, since we refer to the ordering of the Eu^{2+} moments in the ab plane, i.e., to the interlayer coupling. Measuring along the c axis,

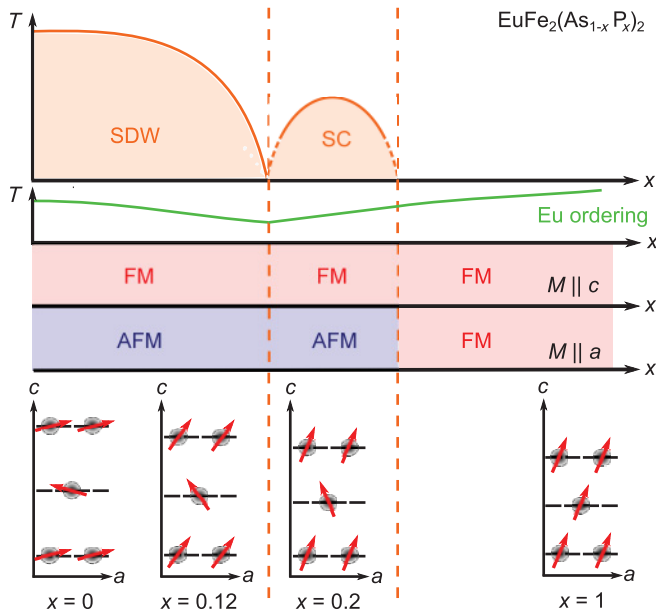


FIG. 4. (Color online) Schematic phase diagram of $\text{EuFe}_2(\text{As}_{1-x}\text{P}_x)_2$ indicating the SDW and SC phase. In the preceding panels, we show the Eu^{2+} ordering and distinguish between the Eu net magnetization along the a axis ($M \parallel a$) and along the c axis ($M \parallel c$). The scheme of the Eu^{2+} spin alignment is also shown with angles given by Ref. 8 at $T = 5$ K. In the parent compound, A-type AFM is found with the spins being slightly canted with an angle of $13(7)^\circ$ off the ab plane. With pressure, the canting angle increases until it saturates at $68(3)^\circ$, when the SDW is completely suppressed. At even higher pressure, the AFM interlayer coupling turns into a FM one.

we yield already a clear FM component for our $x = 0.12$ sample, which is close to the superconducting phase; for this direction, superconductivity coexists with FM. We sketch a phase diagram in Fig. 4, where we distinguish between the Eu net magnetization along the a and c axis. This causes implications that are interesting for theoretical considerations about the interplay of magnetism and superconductivity, as superconductivity in pnictides is often considered as quasi-two-dimensional.

Since the distance between Eu layers is $\approx 6 \text{ \AA}$ and thus rather large for direct exchange,¹³ the interlayer Eu coupling is usually ascribed to the indirect Ruderman-Kittel-Kasuya-Yosida (RKKY) interaction.¹⁰ Mössbauer studies of $\text{EuFe}_2(\text{As}_{1-x}\text{P}_x)_2$ indicate that the more the SDW is suppressed by P substitution, the stronger the Eu spins tilt away from the ab plane.⁸ This is also consistent with our clear hysteresis for $x = 0.12$ ($T_{\text{SDW}} = 105$ K), while we see only small changes between $x = 0$ ($T_{\text{SDW}} = 189$ K) and $x = 0.055$ ($T_{\text{SDW}} = 165$ K). Recent works on Ni- and Co-doped EuFe_2As_2 with suppressed SDW also show the Eu spins being aligned closer to the c axis, leading to the conclusion that the Eu spin orientation is defined by the SDW anisotropy.²¹ Calculations by Akbari, Eremin, and Thalmeier on multiband iron pnictides confirm an influence of the itinerant SDW phase on the RKKY interaction between localized moments.⁹ They show that the spin rotational symmetry is broken by the two-dimensional SDW, which results in an anisotropic RKKY interaction described by an

anisotropic XXZ-type Heisenberg exchange.⁹ This anisotropy is only present in the SDW state and vanishes in the normal state.

According to these calculations, the RKKY interaction oscillates between AFM and FM regimes depending on the details of the Fermi surface and the magnitude of the SDW gap. When going from EuFe_2As_2 to EuAs_2P_2 , the a and c axes decrease by 2.3% and 7.3%, respectively, and the Fermi surface is significantly changed.^{22,23} This explains the change of AFM to FM interlayer coupling at high pressure, which we found by in-plane magnetization measurements of $\text{EuFe}_2(\text{As}_{1-x}\text{P}_x)_2$ single crystals,¹³ here shown representatively for $x = 0.35$. Since chemical^{8,13} and physical^{14–16} pressure have a similar effect on EuFe_2As_2 , we propose magnetization measurements under high pressure along the a and c axes of single crystals, because one can then see directly the change of the interlayer coupling on one sample.

Figure 4 explains our data, but is also consistent with high-field measurements on EuFe_2As_2 :³ while for $H \parallel ab$ and $H \parallel c$ saturation is achieved around 1 T, a step in the magnetization curve appears only for $H \parallel ab$. At low fields, the Eu^{2+} spins start to realign, but keep their AFM orientation in adjacent planes; above a kind of spin-flip field, the orientation of the spins parallel to the external field wins over the AFM interlayer coupling. For $H \parallel c$, however, our model explains the absence of such magnetization behavior, since there is no AFM ordering in the c direction that has to be broken. Furthermore, we predict that the step for $H \parallel ab$ gets weaker with increasing canting angle of the Eu^{2+} spins. For larger canting angles, it gets more and more energetically favorable to orient the spins directly parallel to the external field instead of keeping the AFM ordering. In the case of the FM interlayer coupling, the step completely disappears. Actually, this magnetization dependence is observed for $\text{EuFe}_{2-x}\text{Ni}_x\text{As}_2$, with a weak step in the case of $x = 0.03$, which disappears for higher dopings.¹⁰

Understanding the alignment of the Eu^{2+} magnetic moments will also reveal more information on the interplay between magnetism and superconductivity. One interesting feature appearing in Eu 122 pnictides is a resistivity reentrance in the superconducting phase near the Eu^{2+} ordering temperature.^{11–13,24} In Co-doped Eu 122 compounds with AFM interlayer coupling, this reentrance can be suppressed with $H \parallel ab$, while $H \parallel c$ has no influence on it.^{11,24} There is yet no scientific consensus why superconductivity is destroyed by AFM ordering, while it can coexist with field-induced FM. Nevertheless, our model allows us to explain why $H \parallel c$ has no appreciable influence: it only weakens the spin components in the superconducting ab plane without destroying the AFM ordering itself. It should also be noted that, for several Eu 122 compounds, susceptibility measurements show additional features below the pronounced AFM or FM Eu ordering, which could have the same origin as the resistivity re-entrance.^{8,10,11} We want to point out that Ahmed *et al.*²⁵ observe an enhancement of the spin moment on the Fe $3d$ electrons in $\text{EuFe}_2(\text{As}_{0.73}\text{P}_{0.27})_2$ at $T = 18$ K. Together with the ordered Eu^{2+} moments, the internal magnetic field can then exceed the superconducting upper critical field leading to the reentrance of resistivity.

IV. CONCLUDING REMARKS

Analyzing measurements of the magnetic properties of various Eu 122 compounds, we present a scheme of the Eu^{2+} spin alignment in $\text{EuFe}_2(\text{As}_{1-x}\text{P}_x)_2$. The spins are not simply AFM aligned in adjacent ab planes, but canted. The canting increases with pressure, until the SDW in the FeAs layers is suppressed and superconductivity sets in. Superconductivity coexists with AFM interlayer coupling, but the canting causes

an appreciable FM component in c direction. At even higher pressure, the interlayer coupling gets FM.

ACKNOWLEDGMENTS

We thank N. Barišić, R. Beyer, I. Eremin, and Y. Xiao for helpful discussions, the Humboldt Foundation, DFG (SPP1458), and the LGFG BW for financial support.

-
- ¹D. C. Johnston, *Adv. Phys.* **59**, 803 (2010).
²H. S. Jeevan, Z. Hossain, D. Kasinathan, H. Rosner, C. Geibel, and P. Gegenwart, *Phys. Rev. B* **78**, 092406 (2008).
³S. Jiang, Y. Luo, Z. Ren, Z. Zhu, C. Wang, X. Xu, Q. Tao, G. Cao, and Z. Xu, *New J. Phys.* **11**, 025007 (2009).
⁴Y. Xiao, Y. Su, M. Meven, R. Mittal, C. M. N. Kumar, T. Chatterji, S. Price, J. Persson, N. Kumar, S. K. Dhar, A. Thamizhavel, and Th. Brueckel, *Phys. Rev. B* **80**, 174424 (2009).
⁵Y. Xiao, Y. Su, W. Schmidt, K. Schmalzl, C. M. N. Kumar, S. Price, T. Chatterji, R. Mittal, L. J. Chang, S. Nandi, N. Kumar, S. K. Dhar, A. Thamizhavel, and T. Brueckel, *Phys. Rev. B* **81**, 220406(R) (2010).
⁶J. Herrero-Martín, V. Scagnoli, C. Mazzoli, Y. Su, R. Mittal, Y. Xiao, T. Brueckel, N. Kumar, S. K. Dhar, A. Thamizhavel, and L. Paolasini, *Phys. Rev. B* **80**, 134411 (2009).
⁷J. Koo, J. Park, S. K. Cho, K. D. Kim, S.-Y. Park, Y. H. Jeong, Y. J. Park, T. Y. Koo, K.-P. Hong, C.-H. Lee, J.-Y. Kim, B.-K. Cho, K. B. Lee, and H.-J. Kim, *J. Phys. Soc. Jpn.* **79**, 114708 (2010).
⁸I. Nowik, I. Felner, Z. Ren, G. H. Cao, and Z. A. Xu, *J. Phys. Condens. Matter* **23**, 065701 (2011).
⁹A. Akbari, I. Eremin, and P. Thalmeier, *Phys. Rev. B* **84**, 134513 (2011).
¹⁰Z. Ren, X. Lin, Q. Tao, S. Jiang, Z. Zhu, C. Wang, G. Cao, and Z. Xu, *Phys. Rev. B* **79**, 094426 (2009).
¹¹S. Jiang, H. Xing, G. Xuan, Z. Ren, C. Wang, Z. A. Xu, and G. Cao, *Phys. Rev. B* **80**, 184514 (2009).
¹²Z. Ren, Q. Tao, S. Jiang, C. Feng, C. Wang, J. Dai, G. Cao, and Z. Xu, *Phys. Rev. Lett.* **102**, 137002 (2009).
¹³H. S. Jeevan, D. Kasinathan, H. Rosner, and P. Gegenwart, *Phys. Rev. B* **83**, 054511 (2011).
¹⁴C. F. Miclea, M. Nicklas, H. S. Jeevan, D. Kasinathan, Z. Hossain, H. Rosner, P. Gegenwart, C. Geibel, and F. Steglich, *Phys. Rev. B* **79**, 212509 (2009).
¹⁵T. Terashima, M. Kimata, H. Satsukawa, A. Harada, K. Hazama, S. Uji, H. S. Suzuki, T. Matsumoto, and K. Murata, *J. Phys. Soc. Jpn.* **78**, 083701 (2009).
¹⁶K. Matsubayashi, K. Munakata, N. Katayama, M. Isobe, K. Ohgushi, Y. Ueda, N. Kawamura, M. Mizumaki, N. Ishimatsu, M. Hedo, I. Umehara, and Y. Uwatoko, e-print [arXiv:1007.2889](https://arxiv.org/abs/1007.2889).
¹⁷R. Hu, S. L. Bud'ko, W. E. Straszheim, and P. C. Canfield, *Phys. Rev. B* **83**, 094520 (2011).
¹⁸D. Wu, N. Barišić, N. Drichko, S. Kaiser, A. Faridian, M. Dressel, S. Jiang, Z. Ren, L. J. Li, G. H. Cao, Z. A. Xu, H. S. Jeevan, and P. Gegenwart, *Phys. Rev. B* **79**, 155103 (2009).
¹⁹D. Wu, G. Chanda, H. S. Jeevan, P. Gegenwart, and M. Dressel, *Phys. Rev. B* **83**, 100503(R) (2011).
²⁰M. A. Tanatar, A. Kreyssig, S. Nandi, N. Ni, S. L. Bud'ko, P. C. Canfield, A. I. Goldman, and R. Prozorov, *Phys. Rev. B* **79**, 180508(R) (2009).
²¹I. Nowik, I. Felner, Z. Ren, G. H. Cao, and Z. A. Xu, *New J. Phys.* **13**, 023033 (2011).
²²C. Feng, Z. Ren, S. Xu, S. Jiang, Z. A. Xu, G. Cao, I. Nowik, I. Felner, K. Matsubayashi, and Y. Uwatoko, *Phys. Rev. B* **82**, 094426 (2010).
²³S. Thirupathiah, E. D. L. Rienks, H. S. Jeevan, R. Ovsyannikov, E. Slooten, J. Kaas, E. van Heumen, S. de Jong, H. A. Duerr, K. Siemensmeyer, R. Follath, P. Gegenwart, M. S. Golden, and J. Fink, *Phys. Rev. B* **84**, 014531 (2011).
²⁴Y. He, T. Wu, G. Wu, Q. J. Zheng, Y. Z. Liu, H. Chen, J. J. Ying, R. H. Liu, X. F. Wang, Y. L. Xie, Y. J. Yan, J. K. Dong, S. Y. Li, and X. H. Chen, *J. Phys. Condens. Matter* **22**, 235701 (2010).
²⁵A. Ahmed, M. Itou, S. Xu, Z. Xu, G. Cao, Y. Sakurai, J. Penner-Hahn, and A. Deb, *Phys. Rev. Lett.* **105**, 207003 (2010).